# A NEW MULTI-PASSBAND FILTER SYNTHESIS TECHNIQUE

**Mofei Guo[1]*, Michael J. Lancaster[2]*, Costas Constantinou[3]***

*School of Electronics, Electrical and System Engineering, the University of Birmingham, Birmingham, B15 2TT, U.K.

[1] mxg848@bham.ac.uk, [2] m.j.lancaster@bham.ac.uk, [3] c.constantinou@bham.ac.uk

***Abstract:***

*This paper looks at a new design method for resonator-based multi-passband filters. The technique is able to design an arbitrary number of passbands. The design procedure is based on calculating the coupling matrix for a particular topology of coupled resonators. The physical design parameters, such as the centre frequency of each resonator, the coupling between resonators and the external Q-factors can all be analytically synthesised from the filter specifications. In the paper we will show designs for both Chebyshev and quasi-elliptic multi-passband filters. Theoretically, this method can produce any number of passbands where each band shares the same shape.*

*Two simulated and one measured example of filters designed through this method are given; the three examples are: (1) A 10th order uneven bandwidth five-passband filter with Chebyshev response; (2) A 20th order uneven bandwidth five-passband filter with quasi-elliptic response; (3) Measured results from a 4th order dual-passband waveguide resonator based filter.*

## I. INTRODUCTION

Conventionally, the low-pass prototype Chebyshev response can be mapped into a higher frequency band with the well-known frequency transformation technique. This can be done using [1].

$$\Omega = B(\omega) = \frac{\omega_0}{BW}\left(\frac{\omega}{\omega_0} - \frac{\omega_0}{\omega}\right) \qquad \text{Equation 1}$$

where $\omega$ is the frequency variable for de-normalised response; $\Omega$ is the normalised frequency variable for low-pass prototype response; $\omega_0$ is the centre frequency of the de-normalised passband; $BW$ is the bandwidth of the passband (equal ripple bandwidth for Chebyshev response).

Figure 1 gives a illustrative view of the de-normalised procedure based on Equation 1. In the figure, $\omega_L$ and $\omega_H$ are the lower and higher band limits for de-normalised passband, respectively.

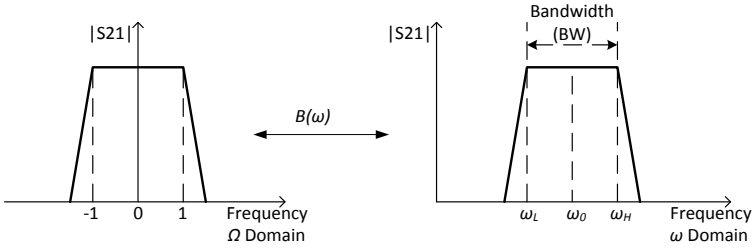


Figure 1. The conventional de-normalised procedure for bandpass filter

Now, let us consider a situation, by applying a new frequency transformation formula $M(\omega)$, the low-pass prototype response can be mapped into multiple higher frequency bands in the de-

normalised procedure. Figure 2 gives an illustrative view of this procedure, showing $\omega_{Li}$ and $\omega_{Hi}$ ($i$=1,2,3,...,$M$) are the band limits for $i^{th}$ passband on the de-normalised response.

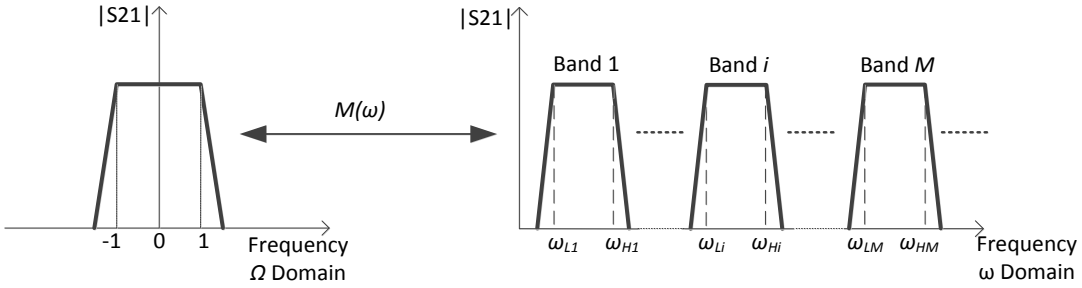


Figure 2. The de-normalised procedure for multi-passband filter

This paper aims to present the multi-passband filter synthesis technique step by step. A new generalised approach of multi-passband filter design is given. It allows the number of passband and the bandwidth of each individual passband to be set as an arbitrary value. With given band limits of each passband, and specifications of the low-pass prototype response, a multi-passband response can be generated with coupling matrix and external Q-factors synthesised at the same time. Some design examples of multi-passband filters with corresponding frequency transformation formulas which are based on this approach are presented.

## II. GENERALISED INVERTER COUPLED RESONATOR SECTIONS

The synthesis techniques for multi-passband filter will be discussed from the topology point of view. Before that, the concept of inverter coupled resonator sections is introduced. They are called inverter coupled resonator sections, since the resonators in each section are coupled by inverters. Basically, the inverter coupled resonator section can be categorised into three types which are shown in Figure 3. For the first type, all bandstop resonators are directly connected to the bandpass resonator; it is named as parallel coupled resonator section. For the second type, the bandstop resonators have an inline layout and only one bandstop resonator is directly connected to the bandpass resonator; it is named as series coupled resonator section. The third one is the mixed coupled resonator section which contains both parallel and series couple resonator at the same time. The bigger circles represent bandpass resonators; the smaller circles represent bandstop resonators; the solid lines stand for couplings between resonators; the dashed lines mean some unshown re-occurring parts.

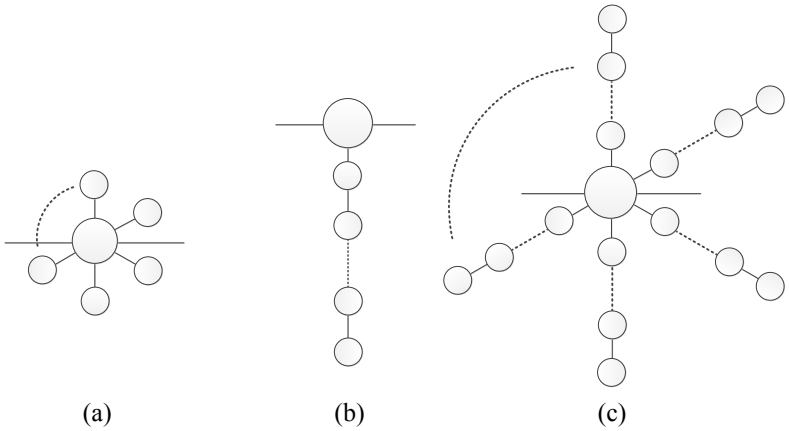


Figure 3. Different kind of inverter coupled resonator sections: (a) parallel, (b) series, (c) mixed

The multi-passband filters we discussed here are built up with these sections. For each section, there is only one bandpass resonator, but the number of bandstop resonator is not limited. Within one particular multi-passband filter, all the sections share the same topology; the

repeating sections are connected through the bandpass resonators. It is actually the inverter coupled resonator section that ultimately determines the frequency transformation formula and the multi-passband response in this multi-passband synthesis technique [2].

### *A. PARALELL COUPLED RESONATOR SECTION*

Figure 4 shows a generalised multi-passband filter which is built up by parallel coupled resonator sections. Resonator 1 to *n* are the bandpass resonators. For example, if these *n* bandpass resonators generate an $n^{th}$ order Chebyshev response, then each passband of this multi-passband filter will have the same $n^{th}$ order Chebyshev response.

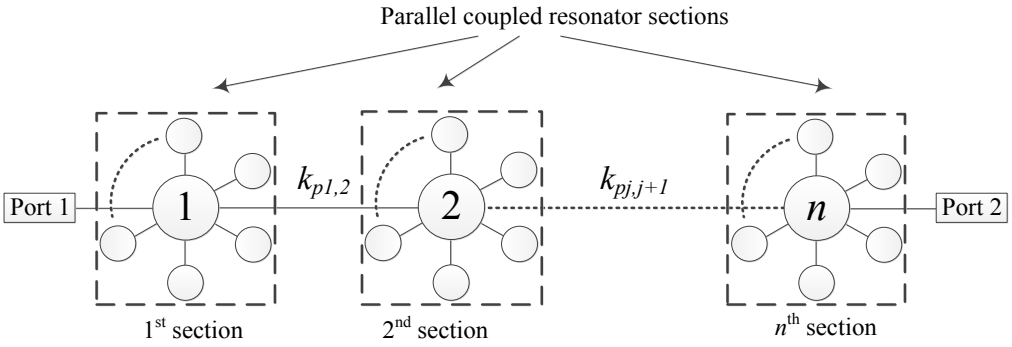


Figure 4. The topology of a generalised multi-passband filter which is built up by parallel coupled resonator sections. The bigger circles represent bandpass resonators; the smaller circles represent bandstop resonators.

The couplings in between bandpass resonators $k_{pj,j+1}$ ($j$=1,2,...,$n$-1) can be calculated by [2],

$$k_{pj,j+1} = \frac{J_{j,j+1}}{b_1}, \qquad J_{j,j+1} = \frac{1}{\sqrt{g_j \cdot g_{j,j+1}}} \ (j=1,2,...,n-1) \qquad \text{Equation 2}$$

in which $J_{j,j+1}$ ($j$=1,2,...,n-1) are the values of $J$-inverters of low-pass prototype filter. In the case of filter with Chebyshev response, they can be obtained from standard Chebyshev filter synthesis procedure that are calculated from $g$-values in Equation 2; $b_1$ is the susceptance slope parameter of the resonators whose centre frequency is $\omega_{o1}$ which can be calculated from [3], in which $C_i$ and $L_i$ are the equivalent capacitance and inductance of $i^{th}$ resonator.

$$b_i = \omega_{oi} \cdot C_i, \qquad \omega_{oi} = \frac{1}{\sqrt{L_i \cdot C_i}} \qquad (i=1,2,3,...,M) \qquad \text{Equation 3}$$

Figure 5 presents a detailed picture of the 1st section of the multi-passband filter that is shown in Figure 4. The multi-passband filter is made up of *n* sections like this. It shows a generalised topology of a single parallel coupled resonator section. *M* is the number of resonators in one parallel coupled resonator section. *M* could be any positive integers. In each resonator section, the bandpass resonator is directly coupled to *M*-1 bandstop resonators. So there will be $M \times n$ resonators in total for the multi-passband filter. $\omega_{oi}$ and $b_i$ ($i$=1,2,3,...,$M$) are the centre frequency and susceptance slope parameter for the $i^{th}$ resonator, respectively. When $i$=1, the resonator is a bandpass resonator; when $i$=2,3,...,$M$, the resonator is a bandstop resonator. All the *n* sections which are shown in Figure 4 share the same layout and parameters.

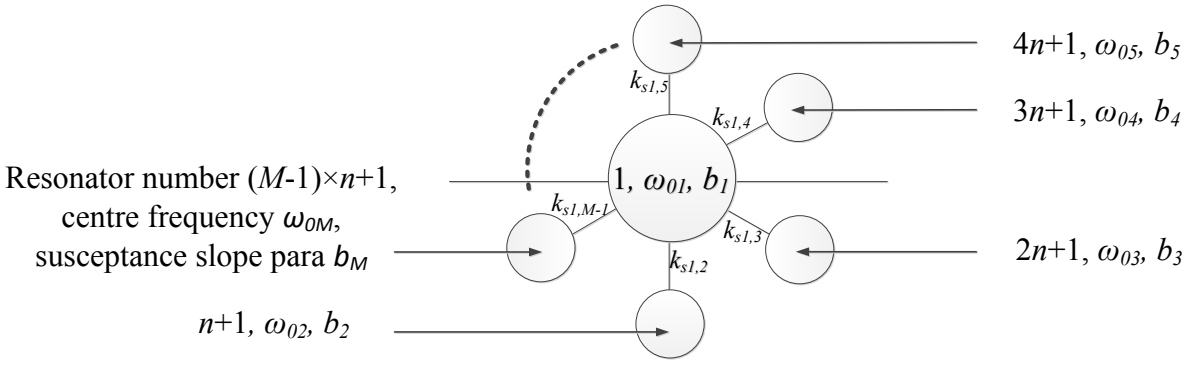


Figure 5. 1st parallel coupled resonator section (*n* is the order of the each passband, *M* is the total number of passbands

The couplings between the bandpass resonator and all bandstop resonators are calculated by

$$k_{s1,i} = \frac{1}{\sqrt{b_1 \cdot b_i}} \ (i=2,3,\ldots,M\text{-}1) \qquad \text{Equation 4}$$

The above equation together with the frequency transformation $M_P(\omega)$ for the multi-passband filter with such parallel coupled resonator sections is based on [2] but generalised,

$$\Omega = M_P(\omega) = b_1\left(\frac{\omega}{\omega_{o1}} - \frac{\omega_{o1}}{\omega}\right) - \frac{1}{b_2\left(\frac{\omega}{\omega_{o2}} - \frac{\omega_{o2}}{\omega}\right)} - \frac{1}{b_3\left(\frac{\omega}{\omega_{o3}} - \frac{\omega_{o3}}{\omega}\right)} - \frac{1}{b_4\left(\frac{\omega}{\omega_{o4}} - \frac{\omega_{o4}}{\omega}\right)} - \frac{1}{b_5\left(\frac{\omega}{\omega_{o5}} - \frac{\omega_{o5}}{\omega}\right)} \cdots\cdots\cdots\cdots \frac{1}{b_M\left(\frac{\omega}{\omega_{oM}} - \frac{\omega_{oM}}{\omega}\right)}$$

Equation 5

By applying Equation 5, the prototype bandpass response can be mapped into *M* different frequency bands. Figure 6 gives an illustrative view of this procedure, in which $\omega_{Li}$ and $\omega_{Hi}$ (*i*=1,2,...,*M*) are the lower and higher passband limits for Band *i* (*i*=1,2,...,*M*), respectively. What should be noticed is that, for the multi-passband filter built up with this parallel coupled resonator sections, the centre frequencies of bandstop resonators $\omega_{oi}$ (*i*=2,3,...,*M*) are also the frequencies of transmission zeros between each band. There are *M* bands in total for this multi-passband filter.

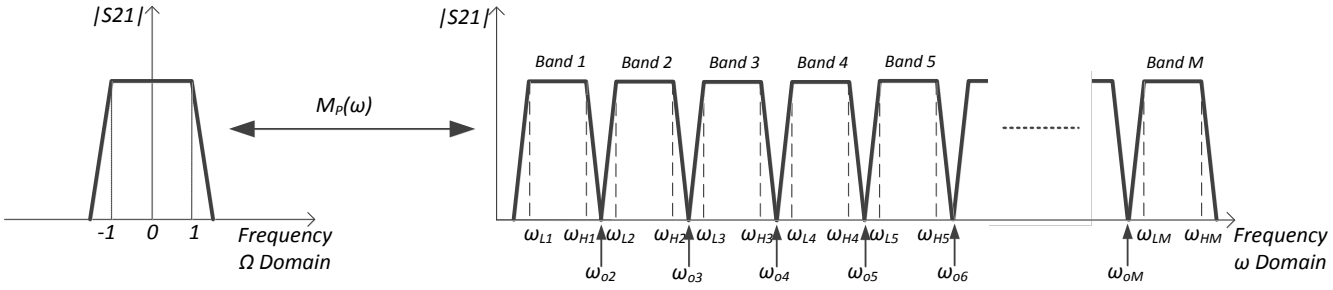


Figure 6. A schematic S21 for multi-passband synthesis technique with parallel coupled resonator section

It should be noted that filter with this topology could have a large number of couplings to each passband resonator, which may be difficult for practical implementation.

### *B. SERIES COUPLED RESOANTOR SECTION*

The topology of a generalised multi-passband filter based on series coupled resonator sections is shown in Figure 7. Again, the resonators from 1 to *n* are the bandpass resonators. These bandpass resonators determine the shape of each passband for this multi-passband filter.

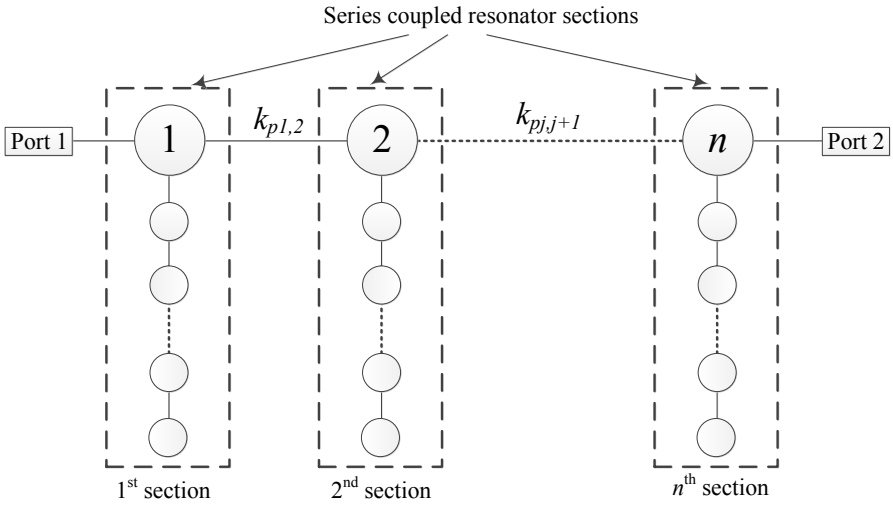


Figure 7. The topology of a generalised multi-passband filter which is built up by series coupled resonator sections. The bigger circles represent bandpass resonators; the smaller circles represent bandstop resonators.

Figure 8 shows the detailed layout of the 1st section in Figure 7. Similar to the previous parallel case, there are also *n* repeating sections in one multi-passband filter. Each section contains one bandpass resonator which resonates at $\omega_{o1}$ and *M*-1 bandstop resonators resonate at $\omega_{oi}$ (*i*=2,3,...,*M*). There are $M \times n$ resonators in this multi-passband filter, as well.

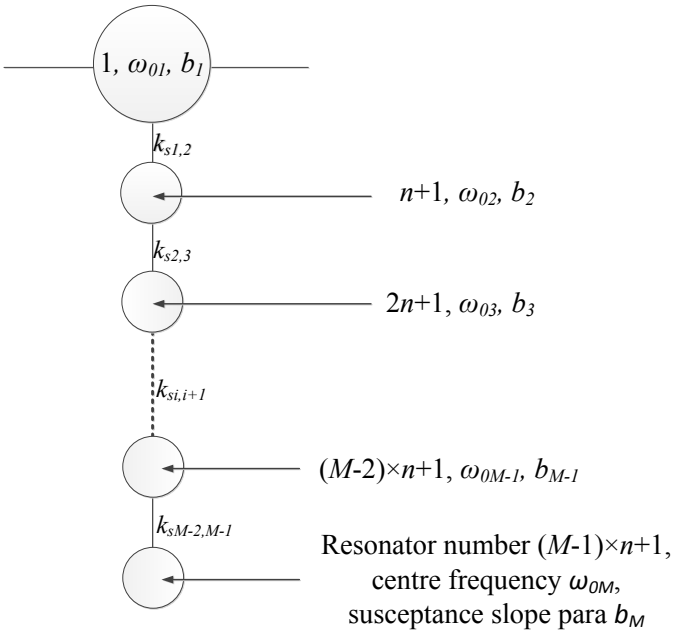


Figure 8. 1st series coupled resonator section (*n* is the order of the each passband, *M* is the total number of passbands)

The couplings between the resonators in one section are defined by,

$$k_{si,i+1} = \frac{1}{\sqrt{b_i \cdot b_{i+1}}} \quad (i=1,2,\ldots,M\text{-}2) \qquad \text{Equation 6}$$

The frequency transformation $M_S(\omega)$ for this series coupled resonator section based multi-passband filter is generalised from [4],

$$\Omega = M_S(\omega) = b_1\left(\frac{\omega}{\omega_{o1}} - \frac{\omega_{o1}}{\omega}\right) - \cfrac{1}{b_2\left(\frac{\omega}{\omega_{o2}} - \frac{\omega_{o2}}{\omega}\right) - \cfrac{1}{b_3\left(\frac{\omega}{\omega_{o3}} - \frac{\omega_{o3}}{\omega}\right) - \ddots - \cfrac{1}{b_{M-1}\left(\frac{\omega}{\omega_{oM-1}} - \frac{\omega_{oM-1}}{\omega}\right) - \cfrac{1}{b_M\left(\frac{\omega}{\omega_{oM}} - \frac{\omega_{oM}}{\omega}\right)}}}}$$

Equation 7

The illustrative procedure of this multi-passband de-normalising process carried out by Equation 7 is shown in Figure 9.

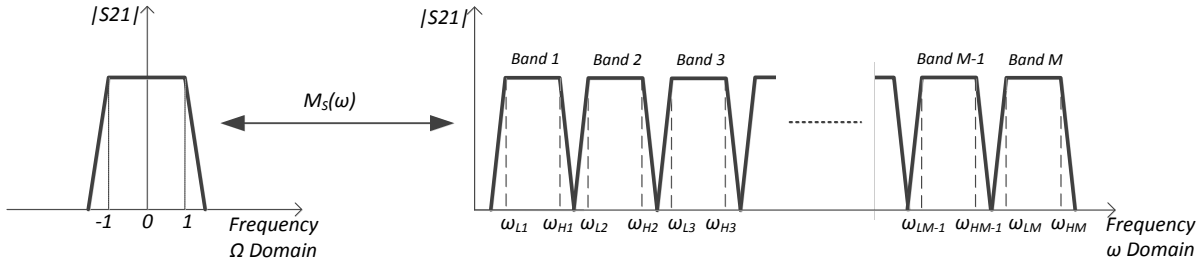


Figure 9. Schematic S21 for multi-passband synthesis technique with series coupled resonator section

There are *M* passbands in total for this multi-passband filter as well. But it should be noticed that, compared to the parallel coupled resonator section based topology, $\omega_{oi}$ ($i$=2,3,…,$M$) are not the transmission zeros between each band anymore; they only act as the centre frequencies of the $i^{th}$ ($i$=2,3,…,$M$) resonator.

### *C. MIXED COUPLED RESONATOR SECTION — AN EXAMPLE FOR FIVE-PASSBAND RESPONSE*

Figure 10 shows a generalised multi-passband filter made up of mixed coupled resonator sections which includes both parallel and series coupled resonator structures. Resonator 1 to resonator *n* are still bandpass resonators, which determine the passband shape in the de-normalised multi-passband response.

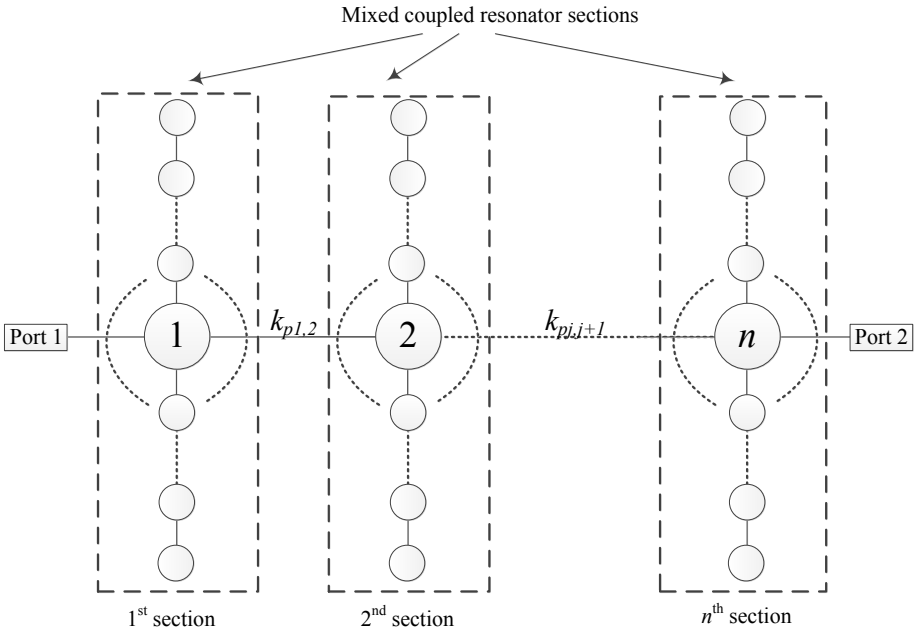


Figure 10. The topology of a generalised multi-passband filter which is built up by mixed coupled resonator sections. The bigger circles represent bandpass resonators; the smaller circles represent bandstop resonators.

Because of the complex in parameter naming, an intuitive example topology of a single mixed coupled resonator section is given in Figure 11, rather than a generalised topology. But it still gives a good indication of the structure.

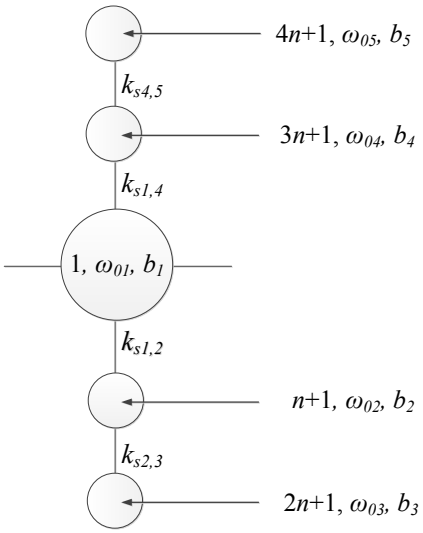


Figure 11. An example of mixed coupled resonator section (for five-passband response)

In Figure 11, resonator 1 is the bandpass resonator; all the other four resonators are bandstop resonators. Two bandstop resonators (resonator $n$+1 and resonator 3$n$+1) are directly connected to the bandpass resonator; while the other two bandstop resonators (resonator 2$n$+1 and resonator 4$n$+1) are connected to the adjacent bandstop resonators. The inter resonator coupling in this mixed coupled section can be calculated using Equation 4 and Equation 6. With this particular kind of mixed couple resonator section, a five-passband filter is given as an example. The frequency transformation for this five-passband filter is

$$\Omega = F(\omega) = b_1\left(\frac{\omega}{\omega_{o1}} - \frac{\omega_{o1}}{\omega}\right) - \cfrac{1}{b_2\left(\frac{\omega}{\omega_{o2}} - \frac{\omega_{o2}}{\omega}\right) - \cfrac{1}{b_3\left(\frac{\omega}{\omega_{o3}} - \frac{\omega_{o3}}{\omega}\right)}} - \cfrac{1}{b_4\left(\frac{\omega}{\omega_{o4}} - \frac{\omega_{o4}}{\omega}\right) - \cfrac{1}{b_5\left(\frac{\omega}{\omega_{o5}} - \frac{\omega_{o5}}{\omega}\right)}}$$

Equation 8

The corresponding frequency transformation procedure is presented in Figure 12.

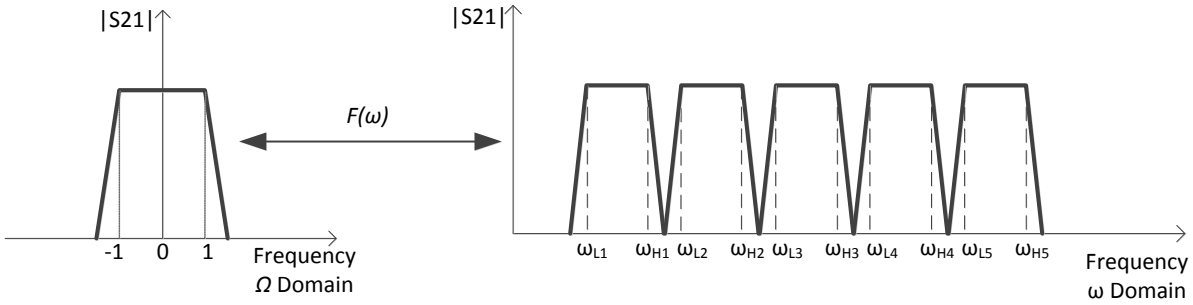


Figure 12. Schematic S21 for five-passband synthesis technique with mixed coupled resonator section

Specified examples are given in next section to validate the general theory of multi-passband filter synthesis technique which is proposed here.

## III. SIMULATED AND MEASURED MULTI-PASSBAND FILTER EXAMPLES

To validate the synthesis technique, two examples of five-passband filters with simulated results are given. In addition, one example of dual-passband filters with measured result is given. The first is a 10th order uneven bandwidth five-passband filter with Chebyshev response (simulated). This is followed by another more complex example of a 20th order uneven bandwidth five-passband filter with quasi-elliptic response (simulated); this shows the flexibility of the synthesis technique. A fabricated 4th order dual-passband filter with Chebyshev response (measured) is given at the end of the paper.

### *A. EXAMPLE 1: A 10TH ORDER UNEVEN BANDWIDTH FIVE-PASSBAND FILTER WITH CHEBYSHEV RESPONSE (SIMULATED RESULT)*

Figure 13 shows a 10th order five-passband filter which is built up with the mixed coupled resonator sections shown in Figure 11.

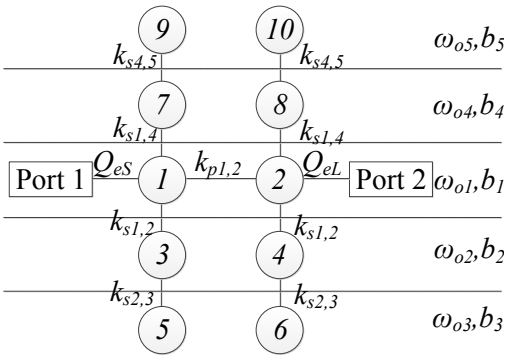


Figure 13. The topology of a 10th order five-passband filter (each passband has a 2nd order Chebyshev response)

The frequency transformation in Equation 8 maps $\omega_{Li}$ and $\omega_{Hi}$ ($i$=1,2,3,4,5) on the de-normalised frequency domain to -1 and 1 on normalised frequency domain (see Figure 12), this process can be interpreted as,

$$\begin{aligned} &F(-\omega_{L1}) = F(-\omega_{L2}) = F(-\omega_{L3}) = F(-\omega_{L4}) = F(-\omega_{L5}) \\ &= F(\omega_{H1}) = F(\omega_{H2}) = F(\omega_{H3}) = F(\omega_{H4}) = F(\omega_{H5}) = 1 \end{aligned} \quad \text{Equation 9}$$

let

$$VF(\omega) = F(\omega) - 1 \quad \text{Equation 10}$$

Now, $\omega_{Li}$ and $\omega_{Hi}$ ($i$=1,2,3,4,5) are the zeros of $VF(\omega)$, while $VF(\omega)$ can also be expressed in terms of polynomial as,

$$VF(\omega) = \frac{ZF(\omega)}{PF(\omega)} = \frac{\omega^{10} + z_9\omega^9 + z_8\omega^8 + z_7\omega^7 + z_6\omega^6 + z_5\omega^5 + z_4\omega^4 + z_3\omega^3 + z_2\omega^2 + z_1\omega + z_0}{p_9\omega^9 + p_8\omega^8 + p_7\omega^7 + p_6\omega^6 + p_5\omega^5 + p_4\omega^4 + p_3\omega^3 + p_2\omega^2 + p_1\omega + p_0} \quad \text{Equation 11}$$

$ZF(\omega)$ and $PF(\omega)$ are the nominator and denominator of the $VF(\omega)$, respectively. As shown in Equation 11, they are expressed in terms of polynomials; $z_i$ ($i$=0,1,...,9) are the normalised coefficients of $ZF(\omega)$; $p_i$ ($i$=0,1,...,9) are the coefficients of $PF(\omega)$.

By using Equation 8, Equation 10 and Equation 11, $z_i$ ($i$=0,1,...,9) can be obtained in terms of $\omega_{oi}$ and $b_i$ ($i$=1,2,3,4,5). Meanwhile, $-\omega_{Li}$ and $\omega_{Hi}$ ($i$=1,2,3,4,5) are the zeros of $VF(\omega)$. Therefore, $z_i$ ($i$=0,1,...,9) can also be obtained in terms of $\omega_{Li}$ and $\omega_{Hi}$ ($i$=1,2,3,4,5) from the equation below,

$$\begin{aligned} &\omega^{10} + z_9\omega^9 + z_8\omega^8 + z_7\omega^7 + z_6\omega^6 + z_5\omega^5 + z_4\omega^4 + z_3\omega^3 + z_2\omega^2 + z_1\omega + z_0 = \\ &(\omega+\omega_{L1})\cdot(\omega+\omega_{L2})\cdot(\omega+\omega_{L3})\cdot(\omega+\omega_{L4})\cdot(\omega+\omega_{L5})\cdot(\omega-\omega_{H1})\cdot(\omega-\omega_{H2})\cdot(\omega-\omega_{H3})\cdot(\omega-\omega_{H4})\cdot(\omega-\omega_{H5}) = 0 \end{aligned}$$

Equation 12

A 10th order equation set which only contains $\omega_{oi}$, $b_i$, $\omega_{Li}$ and $\omega_{Hi}$ ($i$=1,2,3,4,5) has been established. Therefore, $\omega_{oi}$ and $b_i$ ($i$=1,2,3,4,5) can be derived with given $\omega_{Li}$ and $\omega_{Hi}$ ($i$=1,2,3,4,5). Hence, the five-passband frequency transformation in Equation 8 is fully defined.

A numerical example is given below. This example is based on the topology shown in Figure 13. The passband limits and corresponding design parameters are given in Table 1. The design parameters are obtained from passband limits by using the theory proposed above.

| **Passband limits** | **Design parameters** |
|---|---|
| $\omega_{L1}$=9.20 GHz | $\omega_{o1}$=9.94 GHz |
| $\omega_{H1}$=9.29 GHz | $\omega_{o2}$=9.59 GHz |
| $\omega_{L2}$=9.41 GHz | $\omega_{o3}$=9.43 GHz |
| $\omega_{H2}$=9.67 GHz | $\omega_{o4}$=10.35 GHz |
| $\omega_{L3}$=9.80 GHz | $\omega_{o5}$=10.43 GHz |
| $\omega_{H3}$=10.17 GHz | $b_1$=9.22 |
| $\omega_{L4}$=10.25 GHz | $b_2$=51.88 |
| $\omega_{H4}$=10.48 GHz | $b_3$=12.16 |
| $\omega_{L5}$=10.57 GHz | $b_4$=78.94 |
| $\omega_{H5}$=10.70 GHz | $b_5$=13.30 |

Table 1. The passband limits and design parameters for five-passband filter

The corresponding coupling matrix is defined below,

$$[M]=\begin{pmatrix} k_{1,1} & k_{p1,2} & k_{s1,2} & 0 & 0 & 0 & k_{s1,4} & 0 & 0 & 0 \\ k_{p1,2} & k_{2,2} & 0 & k_{s1,2} & 0 & 0 & 0 & k_{s1,4} & 0 & 0 \\ k_{s1,2} & 0 & k_{3,3} & 0 & k_{s2,3} & 0 & 0 & 0 & 0 & 0 \\ 0 & k_{s1,2} & 0 & k_{4,4} & 0 & k_{s2,3} & 0 & 0 & 0 & 0 \\ 0 & 0 & k_{s2,3} & 0 & k_{5,5} & 0 & 0 & 0 & 0 & 0 \\ 0 & 0 & 0 & k_{s2,3} & 0 & k_{6,6} & 0 & 0 & 0 & 0 \\ k_{s1,4} & 0 & 0 & 0 & 0 & 0 & k_{7,7} & 0 & k_{s4,5} & 0 \\ 0 & k_{s1,4} & 0 & 0 & 0 & 0 & 0 & k_{8,8} & 0 & k_{s4,5} \\ 0 & 0 & 0 & 0 & 0 & 0 & k_{s4,5} & 0 & k_{9,9} & 0 \\ 0 & 0 & 0 & 0 & 0 & 0 & 0 & k_{s4,5} & 0 & k_{10,10} \end{pmatrix}$$

Equation 13

The non-diagonal elements in the matrix (inter-resonator couplings) can be calculated using Equation 2, Equation 3 and Equation 6; the diagonal elements (self-couplings) can be calculated with the following equation, in which $f_{0i}$ is the resonant frequency of $i^{th}$ resonator, $f_0$ is the centre frequency of the filter.

$$k_{i,i}=\left(\frac{f_{0i}}{f_0}-\frac{f_0}{f_{0i}}\right) \qquad \text{Equation 14}$$

The external $Q$-factors can be calculated from,

$$Q_{eS}=\frac{b_1}{J_{S1}^{\ 2}}=b_1\cdot g_0\cdot g_1,\quad Q_{eL}=\frac{b_1}{J_{nL}^{\ 2}}=b_1\cdot g_n\cdot g_{n+1} \qquad \text{Equation 15}$$

For this example, the coupling matrix and external $Q$-factors are calculated below,

$$[M]=\begin{pmatrix} -0.0020 & 0.1803 & 0.0457 & 0 & 0 & 0 & 0.0371 & 0 & 0 & 0 \\ 0.1803 & -0.0020 & 0 & 0.0457 & 0 & 0 & 0 & 0.0371 & 0 & 0 \\ 0.0457 & 0 & -0.0737 & 0 & 0.0398 & 0 & 0 & 0 & 0 & 0 \\ 0 & 0.0457 & 0 & -0.0737 & 0 & 0.0398 & 0 & 0 & 0 & 0 \\ 0 & 0 & 0.0398 & 0 & -0.1074 & 0 & 0 & 0 & 0 & 0 \\ 0 & 0 & 0 & 0.0398 & 0 & -0.1074 & 0 & 0 & 0 & 0 \\ 0.0371 & 0 & 0 & 0 & 0 & 0 & 0.0788 & 0 & 0.0309 & 0 \\ 0 & 0.0371 & 0 & 0 & 0 & 0 & 0 & 0.0788 & 0 & 0.0309 \\ 0 & 0 & 0 & 0 & 0 & 0 & 0.0309 & 0 & 0.0943 & 0 \\ 0 & 0 & 0 & 0 & 0 & 0 & 0 & 0.0309 & 0 & 0.0943 \end{pmatrix}$$

$$Q_{eS} = Q_{eL} = 6.13$$

The circuit below is a waveguide implementation of the discussed 10th order five-passband filter with Chebyshev response simulated in CST microwave studio [5]. More details of how to use coupling matrix to generate such a waveguide filter is given in [6].

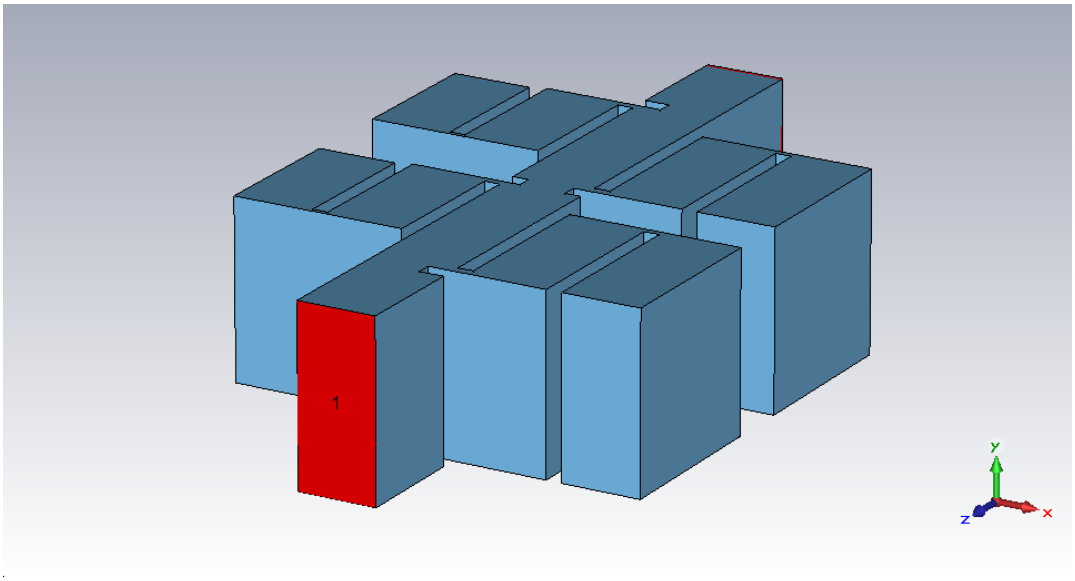


Figure 14. Waveguide implementation of 10th order five-passband filter (Chebyshev); the blue solid represents the air filling of the waveguide which is surrounded by perfect electric conductor. The red plane is the input port; the output port is placed at the other end.

The simulated S21 and S11 together with the calculated S11 are plotted in Figure 15. The simulated results show a good agreement with the calculated one.

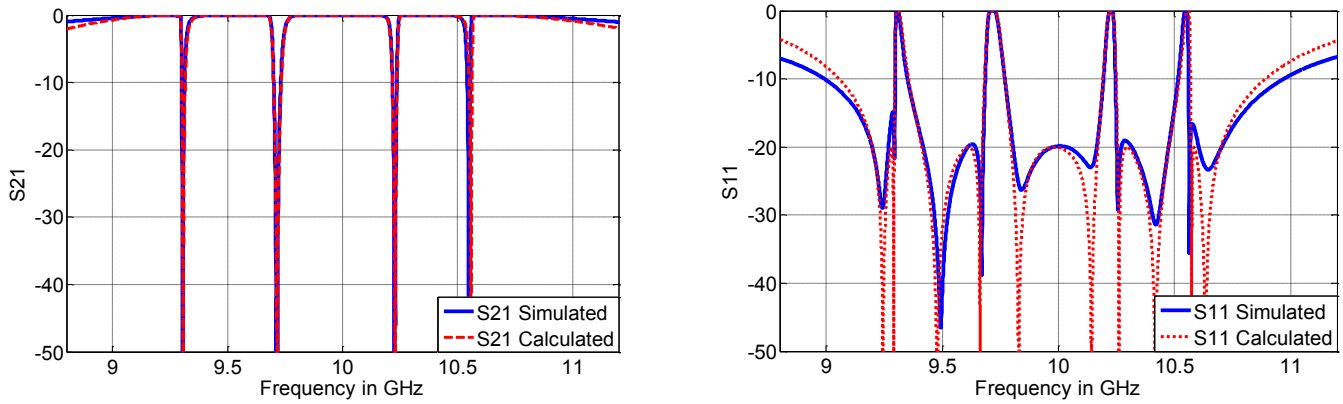


Figure 15. The S-parameter of a 10th order even bandwidth five-passband filter with Chebyshev response (Passband 1: 9.20 ~ 9.29 GHz, Passband 2: 9.41 ~ 9.67 GHz, Passband 3: 9.80 ~ 10.17 GHz, Passband 4: 10.25 ~ 10.48 GHz, Passband 5: 10.57 ~ 10.70 GHz)

### *B. EXAMPLE 2: A 20TH ORDER UNEVEN BANDWIDTH FIVE-PASSBAND FILTER WITH QUASI-ELLIPTIC RESPONSE (SIMULATED RESULT)*

This example is based on a 20th order five-passband filter topology shown in Figure 16. The five passbands are same as that in Example A, i.e. the design parameters are same as well (refer to Table 1). The difference is that in this example, each passband has a 4th order quasi-elliptic response with 20dB maximum return loss.

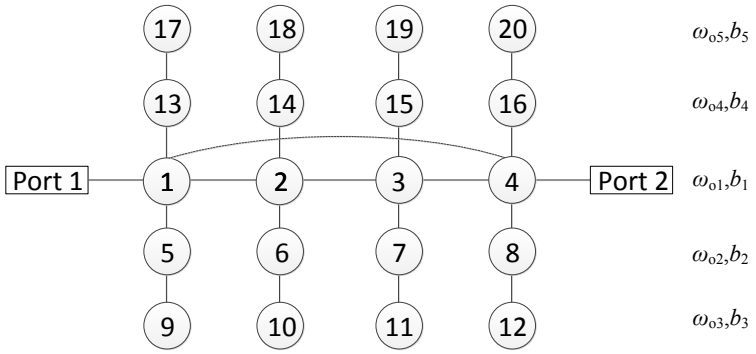


Figure 16. The topology of a 20th order five-passband filter (each passband has a 4th order quasi-elliptic response)

The corresponding coupling matrix can be calculated using Equation 2, Equation 3, Equation 6 and Equation 14. The external *Q*-factors can be obtained from Equation 15. The results are shown below,

$$[M]=\begin{pmatrix}
-0.0020 & 0.0901 & 0 & -0.0321 & 0.0457 & 0 & 0 & 0 & 0 & 0 & 0 & 0 & 0.0371 & 0 & 0 & 0 & 0 & 0 & 0 & 0 \\
0.0901 & -0.0020 & 0.0883 & 0 & 0 & 0.0457 & 0 & 0 & 0 & 0 & 0 & 0 & 0 & 0.0371 & 0 & 0 & 0 & 0 & 0 & 0 \\
0 & 0.0883 & -0.0020 & 0.0901 & 0 & 0 & 0.0457 & 0 & 0 & 0 & 0 & 0 & 0 & 0 & 0.0371 & 0 & 0 & 0 & 0 & 0 \\
-0.0321 & 0 & 0.0901 & -0.0020 & 0 & 0 & 0 & 0.0457 & 0 & 0 & 0 & 0 & 0 & 0 & 0 & 0.0371 & 0 & 0 & 0 & 0 \\
0.0457 & 0 & 0 & 0 & -0.0737 & 0 & 0 & 0 & 0.0398 & 0 & 0 & 0 & 0 & 0 & 0 & 0 & 0 & 0 & 0 & 0 \\
0 & 0.0457 & 0 & 0 & 0 & -0.0737 & 0 & 0 & 0 & 0.0398 & 0 & 0 & 0 & 0 & 0 & 0 & 0 & 0 & 0 & 0 \\
0 & 0 & 0.0457 & 0 & 0 & 0 & -0.0737 & 0 & 0 & 0 & 0.0398 & 0 & 0 & 0 & 0 & 0 & 0 & 0 & 0 & 0 \\
0 & 0 & 0 & 0.0457 & 0 & 0 & 0 & -0.0737 & 0 & 0 & 0 & 0.0398 & 0 & 0 & 0 & 0 & 0 & 0 & 0 & 0 \\
0 & 0 & 0 & 0 & 0.0398 & 0 & 0 & 0 & -0.1074 & 0 & 0 & 0 & 0 & 0 & 0 & 0 & 0 & 0 & 0 & 0 \\
0 & 0 & 0 & 0 & 0 & 0.0398 & 0 & 0 & 0 & -0.1074 & 0 & 0 & 0 & 0 & 0 & 0 & 0 & 0 & 0 & 0 \\
0 & 0 & 0 & 0 & 0 & 0 & 0.0398 & 0 & 0 & 0 & -0.1074 & 0 & 0 & 0 & 0 & 0 & 0 & 0 & 0 & 0 \\
0 & 0 & 0 & 0 & 0 & 0 & 0 & 0.0398 & 0 & 0 & 0 & -0.1074 & 0 & 0 & 0 & 0 & 0 & 0 & 0 & 0 \\
0.0371 & 0 & 0 & 0 & 0 & 0 & 0 & 0 & 0 & 0 & 0 & 0 & 0.0788 & 0 & 0 & 0 & 0.0309 & 0 & 0 & 0 \\
0 & 0.0371 & 0 & 0 & 0 & 0 & 0 & 0 & 0 & 0 & 0 & 0 & 0 & 0.0788 & 0 & 0 & 0 & 0.0309 & 0 & 0 \\
0 & 0 & 0.0371 & 0 & 0 & 0 & 0 & 0 & 0 & 0 & 0 & 0 & 0 & 0 & 0.0788 & 0 & 0 & 0 & 0.0309 & 0 \\
0 & 0 & 0 & 0.0371 & 0 & 0 & 0 & 0 & 0 & 0 & 0 & 0 & 0 & 0 & 0 & 0.0788 & 0 & 0 & 0 & 0.0309 \\
0 & 0 & 0 & 0 & 0 & 0 & 0 & 0 & 0 & 0 & 0 & 0 & 0.0309 & 0 & 0 & 0 & 0.0943 & 0 & 0 & 0 \\
0 & 0 & 0 & 0 & 0 & 0 & 0 & 0 & 0 & 0 & 0 & 0 & 0 & 0.0309 & 0 & 0 & 0 & 0.0943 & 0 & 0 \\
0 & 0 & 0 & 0 & 0 & 0 & 0 & 0 & 0 & 0 & 0 & 0 & 0 & 0 & 0.0309 & 0 & 0 & 0 & 0.0943 & 0 \\
0 & 0 & 0 & 0 & 0 & 0 & 0 & 0 & 0 & 0 & 0 & 0 & 0 & 0 & 0 & 0.0309 & 0 & 0 & 0 & 0.0943
\end{pmatrix}$$

$$Q_{eS} = Q_{eL} = 8.92$$

The component shown in Figure 17 is a simulated waveguide implementation of the 20th order five-passband filter with quasi-elliptic response.

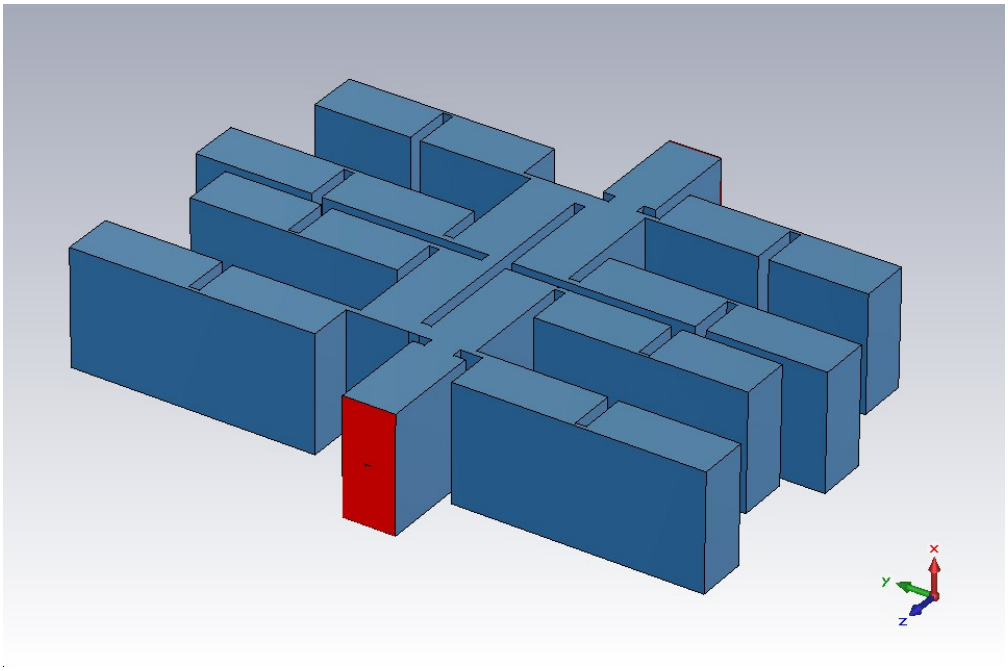

Figure 17. Waveguide implementation of 20th order five-passband filter (quasi-elliptic); the blue solid represents the air filling of the waveguide which is surrounded by perfect electric conductor. The red plane is the input port; the output port is placed at the other end.

The simulated S21 and S11 together with the calculated S11 are plotted in Figure 18,

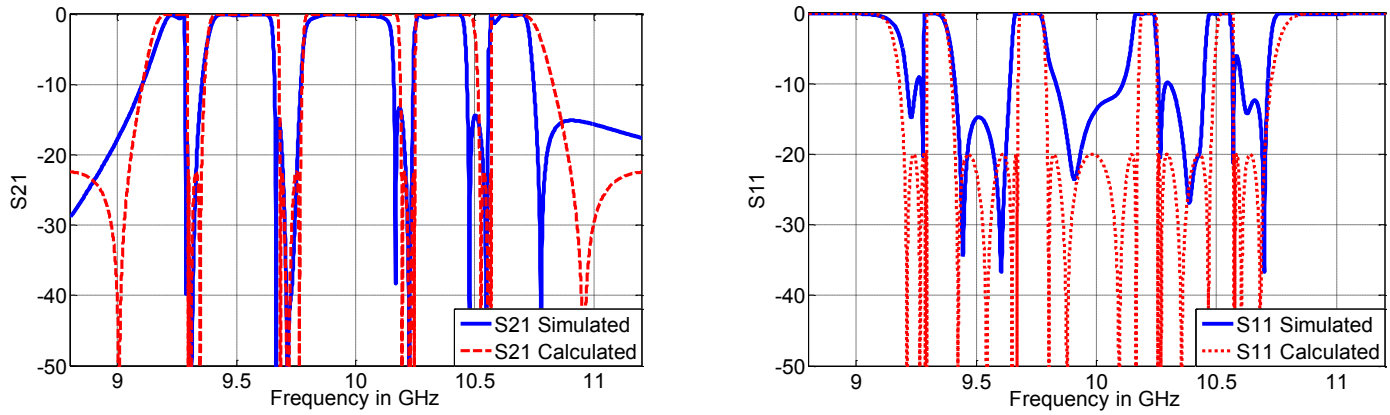


Figure 18. The S-parameter of a 20th order uneven bandwidth five-passband filter with quasi-elliptic response (Passband 1: 9.20 ~ 9.29 GHz, Passband 2: 9.41 ~ 9.67 GHz, Passband 3: 9.80 ~ 10.17 GHz, Passband 4: 10.25 ~ 10.48 GHz, Passband 5: 10.57 ~ 10.70 GHz)

The mismatch of S-parameter in the CST simulation is mainly due to the physical limitations of the waveguide circuit. As one resonator is coupled to up to 4 neighbour resonators at the same time, uncontrolled cross-couplings between non adjacent resonators may occur. Further works will improve the results. The uncontrolled cross-couplings might be further attenuated by re-arranging the circuit layout.

### *C. EXAMPLE 3: A 4TH ORDER UNEVEN BANDWIDTH DUAL-PASSBAND FILTER WITH CHEBYSHEV RESPONSE (MEASURED RESULT)*

The 4th order dual-passband filter has a following topology; the corresponding frequency transformation is given in Equation 16. This example has two uneven passbands (refer to Table 2). Each passband has a 2nd order Chebyshev response with 20dB maximum return loss.

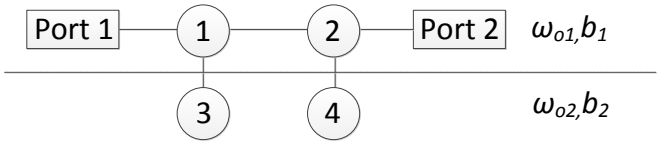


Figure 19. The topology of a 4th order dual-passband filter

$$\Omega = D(\omega) = b_1\left(\frac{\omega}{\omega_{o1}} - \frac{\omega_{o1}}{\omega}\right) - \frac{1}{b_2\left(\frac{\omega}{\omega_{o2}} - \frac{\omega_{o2}}{\omega}\right)} \qquad \text{Equation 16}$$

The passband limits and corresponding design parameters are given in Table 2.

| **Passband limits** | **Design parameters** |
|---|---|
| $\omega_{L1}$=8.65 GHz | $\omega_{o1}$=8.74 GHz |
| $\omega_{H1}$=8.78 GHz | $\omega_{o2}$=8.81 GHz |
| $\omega_{L2}$=8.82 GHz | $b_1$=54.61 |
| $\omega_{H2}$=8.85 GHz | $b_2$=291.7 |

Table 2. The filter specifications and design parameters for dual-passband filter

The corresponding coupling matrix and external $Q$-factors can be calculated using Equation 2, Equation 3, Equation 14 and Equation 15; the results are given below,

$$[M] = \begin{pmatrix} -0.0023 & 0.0304 & 0.0079 & 0 \\ 0.0304 & -0.0023 & 0 & 0.0079 \\ 0.0079 & 0 & 0.0137 & 0 \\ 0 & 0.0079 & 0 & 0.0137 \end{pmatrix}$$

$$Q_{eS} = Q_{eL} = 36.30$$

Below is the structure of this 4th order filter which produces a dual-passband response; each passband has a 2nd order Chebyshev response.

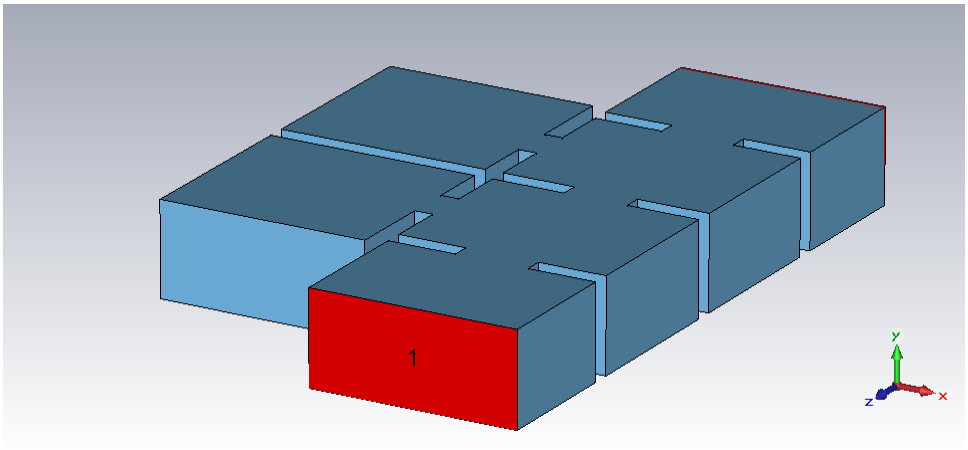


Figure 20. Waveguide implementation of 4th order five-passband filter (Chebyshev); the blue solid represents the air filling of the waveguide which is surrounded by perfect electric conductor. The red plane is the input port; the output port is placed at the other end.

The filter is designed based on the passbands specification shown in Table 2; the measured and calculated S-parameters are plotted below in Figure 21.

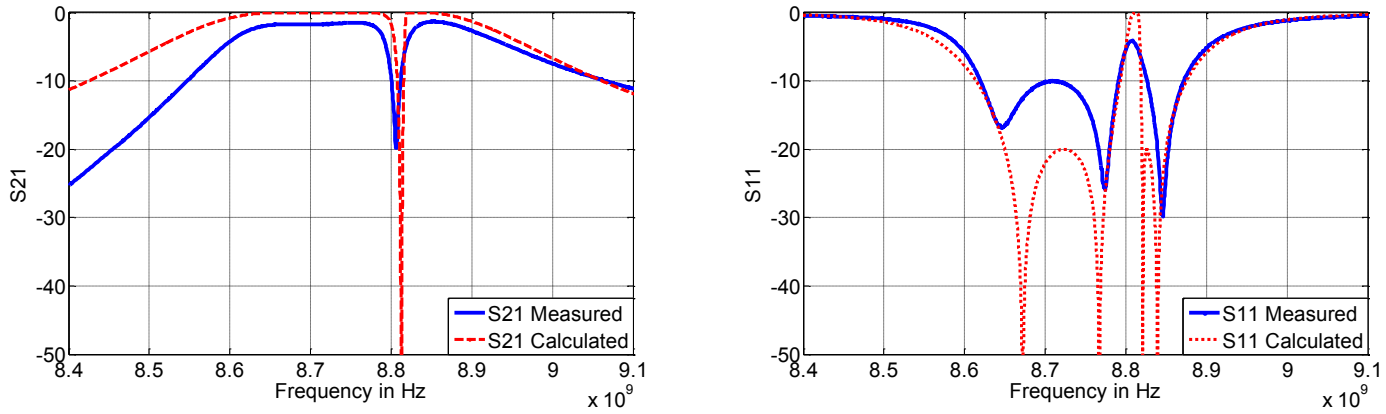


Figure 21. The S-parameter of a 4th order uneven bandwidth dual-passband filter with Chebyshev response (Passband 1: 8.65~ 8.78 GHz, Passband 2: 8.82 ~ 8.85 GHz)

The passband insertion loss is about 1.5dB. It is mainly due to the conductor loss by aluminium and non-perfect construction. Further works on fine tuning may improve the results.

# IV. CONCLUSION

This paper has proposed a generalised analytical synthesis method for multi-passband filter design. The inverter coupled resonator section is the key building block for the multi-passband filter discussed here; within one filter, there is only one kind of inverter coupled resonator section. For one inverter coupled resonator section, there is a unique frequency transformation corresponding to it. The multi-passband response is obtained by applying the frequency transformation to a low-pass prototype response. The number of the resonator in one inverter coupled resonator section is the number of the passbands; the number of the re-occurring inverter coupled resonator section determines the order of the response for each passband.

Two simulated five-passband filters and a measured dual-passband filter are given. They are all designed in X-band and designed in waveguide form. To illustrate the flexibility of this synthesis technique, the three examples all have arbitrary uneven bandwidths; two examples have Chebyshev response, while the other one has quasi-elliptic response. The simulated and measured results show good agreements with the theoretical calculated ones.

# REFERENCES


1. Lancaster, M.J., *passive microwave device applications of high-temperature superconductors.* 1997.
2. Giuseppe Macchiarella, S.T., *Design Techniques for Dual-passband Filters.* IEEE TRANSACTIONS ON MICROWAVE THEORY AND TECHNIQUES, 2005. **53**(11): p. 7.
3. Xiao-Ping Chen, K.W., Zhao-Long Li, *Dual-Band and Triple-Band Substrate Integrated Waveguide Filters With Chebyshev and Quasi-Elliptic Responses.* IEEE TRANSACTIONS ON MICROWAVE THEORY AND TECHNIQUES, 2007. **55**(12): p. 10.
4. Hao Di, B.W., Xin Lai and Chang-Hong Liang, *Synthesis and Realization of Novel Triple-passband Filter Based on Frequency Transformation.* Microwave Conference, 2009, APMC 2009. Asia Pacific, 2009: p. 4.
5. *CST Microwave Studio 2013*, CST - Computer Simulation Technology AG.
6. Shang, X., W. Xia, and M.J. Lancaster, *The design of waveguide filters based on cross-coupled resonators.* Microwave and Optical Technology Letters, 2014. **56**(1): p. 3-8.